2013 IREP Symposium-Bulk Power System Dynamics and Control –IX (IREP), August 25-30, 2013, Rethymnon, Greece

A Simplified Methodology to Estimate the Impact of Wind Power over Operating Reserves in Isolated Power Systems

Luis S. Vargas
Electrical Engineering Department,
Universidad de Chile, Santiago, Chile

Felipe A. Larrain
Electrical Engineering Department,
Universidad de Chile, Santiago, Chile

Abstract

This paper presents a simplified methodology to estimate the impact of wind power over operating reserves in isolated power systems. The methodology is based on a convolution approach that merges the fluctuations of wind speed with the natural variations of demand, and formulates the probability distribution function of variables as a non-Gaussian behavior.

The estimation renders a histogram containing the probability distribution of operating reserves required in different time spans. The methodology also estimates the LOLP indicator to assess the operative reserve of the system. An application on the expansion plan of a Chilean isolated power system is presented and results indicate that the methodology is able to estimate operating reserve needs in a time span ranging from 1 to 30 minutes, which adequately satisfy the future needs of this isolated power system.

I. Introduction

Nowadays in many networks wind power is becoming an important share in electricity supply. As variability is an inherent characteristic of wind power, which has technical and economic implications [1] [2] [3], it has become a crucial problem for the operation of modern power systems.

Wind intermittency may affect the frequency control, particularly in isolated systems with no fast-acting dispatchable sources and without large-scale energy storage systems. In these networks it is important to assess the impact of wind variations on frequency control, particularly the reserve requirements that have to be allocated in the system. Unlike the case of interconnected grids, isolated power systems must ensure enough autonomous reserves in order to compensate any kind of power imbalance that may appear during system operation.

In the northern part of Chile there is an isolated system, the Norte Grande Interconnected System (NGIS), with nearly 2200 MW of peak demand. The wind resources in this location have unique features, such as two peak values in a day; wind vertical profile that does not increase steadily with the height (it starts decreasing after a certain point); and wind speed distribution different from the classic Weibull probability behavior. Also, available wind power has strong competitive advantages against other geographical locations within the region, given its over 30% average plant factor and low seasonal variability [4]. On the other hand, the supply is 98% thermal-based and the demand is mainly mining (more than 80%), therefore there is no much demand variability. Thus, the frequency control mechanisms are slow and with high costs.

This paper describes a simplified methodology for wind power characterization in order to assess the operative reserve for isolated systems. The application of this technique allows modeling the evolution of operative reserves in multiple time scales, an approach that aims at improving power regulation mechanisms design, especially for isolated systems with high wind penetration. The proposed methodology is applied over three wind penetration scenarios of NGIS at 2020.

The remaining of this paper is organized as follows: Chapter II describes the definitions and computation methodologies for operating reserves, Chapter III describes the proposed methodology of this work, Chapter IV presents the case study of the isolated system, Chapter V contains an analysis of the results and Chapter VI summarizes the main conclusions of the paper.

II. Operating Reserve: Definitions and Computation Methodologies

A. Definitions

According to the North American Electric Reliability Corporation (NERC) the operative reserve is the "*capability above firm system demand required to provide*

978-1-4799-0199-9/13/$31.00 ©2013 IEEE

for regulation, load forecasting error, equipment forced and scheduled outages and local area protection. It consists of spinning and non-spinning reserve". In most systems this includes regulation reserve, spinning reserve, supplementary reserve, which are defined in appropriate Control Performance Standards [5] [6].

In Europe, the European Network of Transmission System Operators for Electricity (ENTSO-E) distinguishes reserves for primary, secondary and tertiary control [7]. Primary reserves are allocated to face the most important single event that could threaten the grid, and it is distributed among the generators as a function of their energy production. Secondary reserves aim to satisfy contingencies in generators as well as the natural load variations. Finally, tertiary reserves are used to liberate secondary reserve and to minimize the cost of production and restore the economic dispatch.

In this work the classification proposed by Holttinen et al. [8] is used, which it is shown in Figure 1.

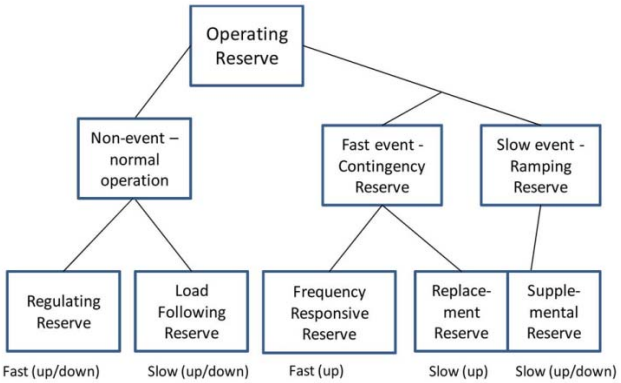

Figure 1. Operating reserves classification diagram.

The concepts of regulating reserve and load following reserve are connected with the study of wind power integration as they are influenced by the incorporation of these types of technologies in the system. To narrow the scope of the concepts, the following definitions are adopted in this study:

> *Regulating Reserve (also known as regulation, load frequency control, primary/secondary control).* Capacity available during normal conditions for assistance in active power balance to correct the current imbalance. Is faster than economic dispatch optimization, is random and requires an automatic centralized response.
>
> *Load Following Reserve (also known as load following, following reserve, tertiary reserve, minute reserve, schedule reserve, dispatch reserve, balancing reserve).* Capacity available during normal conditions for assistance in active power balance to correct a future anticipated imbalance. Does not require an automatic centralized response.

Thus, in a broad sense, primary control-related reserves are fast and provide the first-line corrective action in disturbances; whereas secondary control-related reserves take place on a follow-up time scale and manage the deployment of resources to ensure reliable and economic operation.

As there is a fuzzy line between primary and secondary control-related reserves, which may change with the size and operating conditions of the isolated power systems, in this paper a different approach to define operating reserves is chosen: the proposed methodology aims to assess the required operating reserves for different time spans. Therefore, the concern here is to identify the amount of energy that has to be responsive to the power system operation within a given time window. Whether to classify the time span into primary, secondary or even tertiary reserves is left to the application on the specific isolated power grid.

B. Reserve Computation Methodologies

There is an abundant work done to estimate operative reserve under different wind power penetration scenarios [13-25]. Although the proposed estimation methodologies are different, it is possible to identify two common stages in all of them.

The first stage consists of the estimation of the available wind power. This is usually performed by adopting high temporal and spatial resolution in periods of one to several years. This stage encompasses the future projection of power systems, the availability of wind resources and the selection of suitable locations for wind farms.

In the second stage, the future reserve needs are estimated. Usually this estimation uses a comparative analysis where the cases with and without wind farms are compared. If R_0 is the reserve in the scenario without wind power (Base Scenario), and R is the reserve when the wind farms are in operation in a given time period, operating reserve can be written as $R = R_0 + \Delta R$, where ΔR is the net increment of reserve due to the integration of wind power in the system.

There are deterministic and probabilistic approaches to compute R [8].

The deterministic methodologies compute the reserve as the sum of all components associated to the sources of

variability. Thus, it is common to estimate the reserve as follows:

$$R_0 = R_l + R_c \\ \Delta R = R_w \quad (1)$$

Where R_l is the necessary reserve to cope with the maximum natural demand variation, R_c is the reserve to cope with the most severe contingency, and R_w represents the reserve needed to balance the highest wind power variation in the period.

Among the probabilistic approaches the *n-sigma method* is one of the most popular [8]. This method assumes that demand and wind power are not correlated, and the net increment of reserve is assumed to have a Gaussian Probability Distribution Function (PDF) in the form

$$\Delta R = n\left(\sigma_{net\_error} - \sigma_l\right) \quad (2)$$

where σ_{net_error} is the net variance (superposition of demand and wind power), σ_l is the natural variability of the load and $n = 2.5, 3, 4, or\ 6$.

Another stream of methodologies assumes that the probability distribution function of variables has a non-Gaussian behavior. They generally use the LOLP indicator to assess the operative reserve of the system, which is expressed as a α fraction that covers all possible cases [18]. Formally it is written as

$$\alpha(R) = \mathbb{P}(f(r) * g(r) * h(r) \leq R) \quad (3)$$

and the LOLP function is estimated as

$$LOLP(R) = 1 - \alpha(R) \quad (4)$$

Where: f is the PDF associated to simple contingencies in the grid; g is the PDF associated to the variability of demand; and h is the PDF describing the fluctuations of wind power. The proposed methodology of this work is along this line.

III. Proposed Methodology

The proposed methodology, named Convolution Method, to estimate the required operating reserves for different time spans has three stages:

A. Wind Speed Time Series Estimation
B. Incorporation of Wind Farm Wake Effects
C. Operating Reserve Estimation

A brief description of each stage is presented in this section.

A. Wind Speed Time Series Estimation

Wind profiles are represented by mean values, which are obtained on time windows of 10, 12 or 15 minutes, hereinafter *base interval*, with a yearly scope [26] [27].

In this study, data was obtained from the "Explorador Eólico – Solar" Project, a joint initiative of the Universidad de Chile and the Chilean Government [4]. A spatial resolution of 1 km is used, and a rectangular topology it is assumed for all the wind farms, as shown in Figure 2.

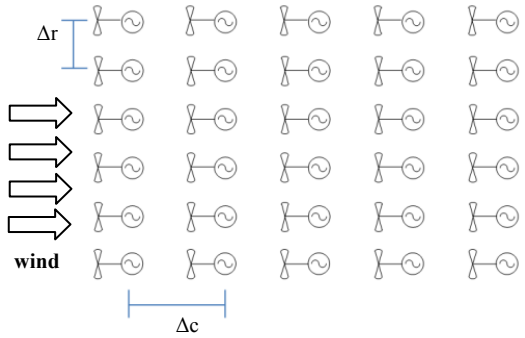

Figure 2. Simplified wind farm block diagram.

In Figure 2 there is a separation of Δc between columns and Δr between rows.

In a given site, wind is the result of a number of weather and geographic conditions. A typical curve representing the Van der Hoven spectrum [28] of wind is shown in Figure 3.

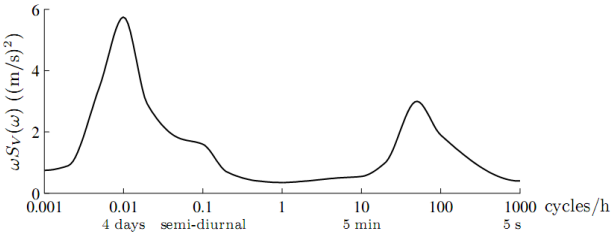

Figure 3. Van der hoven spectrum.

Figure 3 shows that there is a concentration of energy in two distinctive frequencies, which indicates that wind energy may be characterized by mean values, covering a time span of days, and fast variations, called turbulences, covering time spans of seconds to few minutes.

It is common to represent the power spectrum density of turbulences by using the Kaimal approach [29-32]:

$$S_f(f) = \sigma_x^2 \frac{\frac{4L_x}{U_0}}{\left(1 + 6\frac{fL_x}{U_o}\right)^{\frac{5}{3}}} \quad (5)$$

where,

$$\sigma_x = U_0 I \tag{6}$$

$$I = I_{ref}\left(\frac{3}{4} + \frac{5.6}{U_0}\right) \tag{7}$$

$$L_x \cong 8.1 C_x[m] \tag{8}$$

$$C_x \cong 42[m] \tag{9}$$

In equations (5)-(9), $S_f(f)\left[\frac{W}{Hz}\right]$ is the power spectrum density, $U_0\left[\frac{\mathrm{m}}{\mathrm{s}}\right]$ is the average wind speed in the *base interval*, $I[\%]$ is the turbulence intensity, I_{ref} is a reference value (typically between 10% and 20%), $\sigma_x\left[\frac{\mathrm{m}}{\mathrm{s}}\right]$ is the wind standard deviation, $f[Hz]$ is the frequency and L_x is the typical turbulence length.

By using Equation (5) the wind speed is estimated according to the procedure depicted in Figure 4.

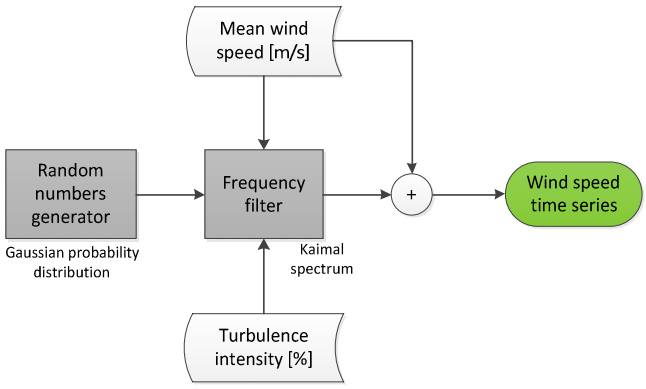

Figure 4. Wind speed time series – building procedure.

Let $v_1(t)$ be the wind speed on the first column, then the wind speed on the second column is obtained from

$$v_2(t+\tau) = v_1(t)\eta(2) \tag{10}$$

where $\tau = \frac{\Delta r}{U_0}$ and $\eta(2)$ is a factor that takes into account the energy extraction of the preceding wind turbines.

The recursive use of Equation (10) leads to an estimation of the entire wind farm. In this computation it is assumed that the wind among different rows is not correlated [30], [33] , [34].

B. Incorporation of Wind Farm Wake Effects

The wake effect on the wind farm has been estimated by using different models, such us in Jensen et al. [35], Frandsen et al. [36], and Ainslie et al. [37]. In this work the Frandsen model is adopted.

The Frandsen model predicts the evolution of the wake effect in two phases: (a) single-wake model (for the second turbine of the row), and (b) multiple-wake model (for the rest of the units) [36].

The equations of the first phase are:

$$\frac{v_2}{v_1} = \frac{1}{2}\left(1 + \sqrt{1 - 2\frac{A_R}{A(x)}C_T}\right) \tag{11}$$

$$A(x) = \frac{\pi}{4}D^2(x) \tag{12}$$

$$D(x) = \left(\beta^{\frac{k}{2}} + \alpha\frac{x}{D_0}\right)^{\frac{1}{k}} D_0 \tag{13}$$

$$A_R = \frac{\pi}{4}D_0^2 \tag{14}$$

$$\beta = \frac{1}{2}\frac{1+\sqrt{1-C_T}}{\sqrt{1-C_T}} \tag{15}$$

$$C_T = 3.5\left(\frac{2v_1^2 - 3.5}{v_1^2}\right) \tag{16}$$

Where $v_1\left[\frac{\mathrm{m}}{\mathrm{s}}\right]$ and $v_2\left[\frac{\mathrm{m}}{\mathrm{s}}\right]$ are the speed of the first and second turbine in a same row, $D_0[m]$ the diameter of the blades, and α and k are fixed parameters (typically $\alpha \in [0.3,0.7]$ and $k = 2$). For the second phase, the conservation of momentum is assumed as:

$$c_{n+1} = 1 - \left(\frac{A_n}{A_{n+1}}(1-c_n) + \frac{A_R}{2A_{n+1}}C_T c_n\right) \tag{17}$$

$$c_n = \frac{U(n)}{U_0} \tag{18}$$

Where A_n and A_{n+1} are the areas covered by the blades.

The wind speed is obtained from the drag law for neutral atmospheric stratification as

$$U(n \gg 1) \approx \frac{kG}{\ln\left(\frac{G}{(f \cdot e^{A_*})z_0}\right)} \tag{19}$$

where: $G\left[\frac{m}{s}\right]$ is the geostrophic wind, $f = 2\Omega\sin\varphi$, is a Coriolis parameter, A_* is a constant depending on latitude and z_0 is a landscape-related parameter.

C. Operating Reserve Estimation

By using the wind speed series from the previous stages the active power generation of wind farms is obtained through the *power vs wind* curve of each turbine-

generator system, which is provided by manufacturers. The wake effect is considered in each wind farm and the total active power generated for each scenario under analysis is completed [30].

Then, by assuming that the demand and wind time series are not correlated, the net impact on operating reserves is computed. A typical curve showing the aggregated effect of demand and wind fluctuations for a given time window is presented in Figure 5.

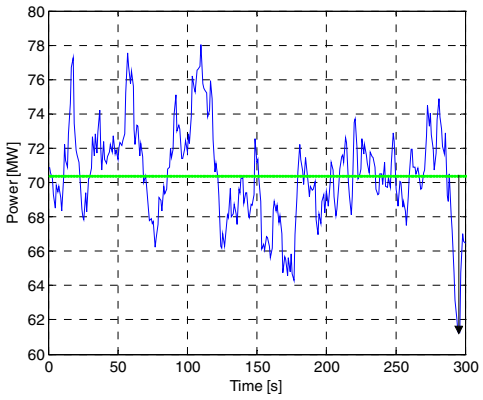

Figure 5. Power time series.

By covering the time window (300 sec in the case of Figure 5), the highest deviation of power is identified. This is performed on all data available and for different time windows. The aggregated result is a histogram containing the power density function of operating reserves required as shown in Figure 6 (for the same time window of 300 sec).

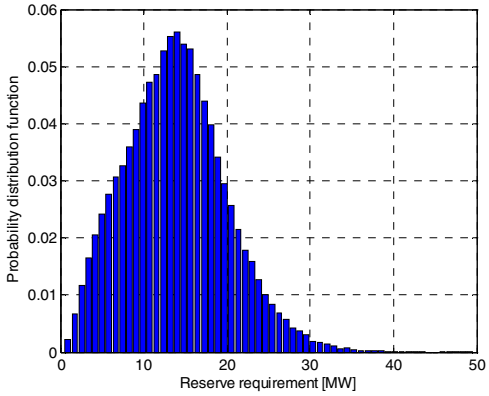

Figure 6. Probability distribution function of operating reserve for a 300 seconds time window.

Thus, for each time window a power density probability distribution function is obtained. Note that as long as data is available, the method may render the corresponding power density probability distribution function for any time window. With this function the operating reserves can be assessed.

IV. Case Study Results: NGIS 2020

The proposed methodology was applied to a small interconnected system located in the north of Chile, the NGIS system, which is shown in Figure 7.

Figure 7. NGIS map and considered wind farms.

The scenarios under study are built on the year 2020 with three different wind power penetration cases: Low, Medium and High integration [38]. The description of each scenario is presented in Table 1.

Table 1. Wind integration scenarios.

LOW INTEGRATION (WF Group A)		**MEDIUM INTEGRATION** (WF Groups A and B)		**HIGH INTEGRATION** (WF Groups A, B and C)	
Installed capacity [MW]	Wind Energy (% of annual demand)	Installed capacity [MW]	Wind Energy (% of annual demand)	Installed capacity [MW]	Wind Energy (% of annual demand)
590	5.94	972	9.77	1332	13.76

Data for the transmission system as well as demand were obtained from the ISO of the NGIS [39] [40]. All wind power generator parameters used in the simulations are obtained from international literature [35] [37].

NGIS has an installed capacity of nearly 4500 MW. Generation, transmission and consumption facilities that

are interconnected from the NGIS cover the northern territory, equivalent to 24.5% of the country's continental territory. NGIS accounts for about 30% of national generation and has a key strategic importance as it provides the energy for the mining activities, which play a significant role in Chile´s economy.

By applying current ISO policies, and with no incorporation of wind power, the expected requirements of primary frequency control (PFC) for NGIS 2020 are 115 MW, whereas the corresponding requirements for secondary frequency control (SFC) are 90[MW].

The Convolution Method was applied to the three scenarios, where the estimated reserve for each time window is able to cover 97% of the critical events in the NGIS system.

A summary of the results for operating reserve's needs, by considering five time windows (1, 5, 10, 20 and 30 minutes), for the three wind penetration scenarios, is shown in Figure 8.

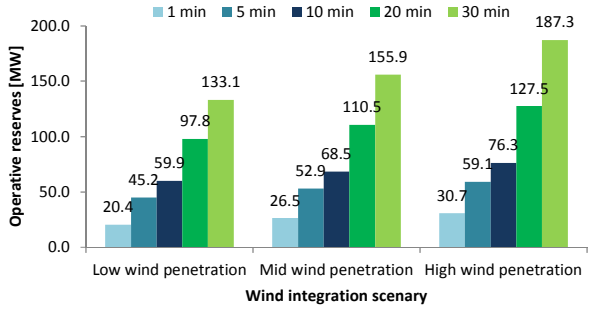

Figure 8. Operating reserve requirements per scenario.

Results of Figure 8 indicate that the greatest operating reserve, by considering wind and natural demand fluctuations, is found for the 30 minutes time window, reaching 133.1[MW] for the Low penetration scenario, 155.9[MW] for Mid penetration scenario, and 187.3[MW] for High penetration scenario (assuming LOLP no greater than 3%).

Thus, when compared to the case where no wind power is considered the net increase in operating reserve requirements for SFC is 97.3 MW (187.3 MW– 90 MW). As NGIS hourly demand will grow up to 3,000[MW] on 2020, thus the operative reserve dedicated to compensate slow unbalances will be around 6% of total demand.

Results also show that the rate of increase in operating reserve is lower than the rate of total wind installed capacity. In fact, by comparing the 30 minutes windows of Low penetration with the High penetration scenario it was found that whereas the wind power installed capacity increased 742 MW (1332 MW - 590 MW), the reserve requirement only increased 54.2 MW (187.3 MW - 133.1 MW). In terms of percentage this means that whereas the installed wind capacity increased a 125.8%, the operating reserve increased only a 40.6%.

These results are in line with the literature on integration of wind power, which reveals that there is no significant impact on operative reserves related to contingencies in a power system, i.e. no significant effect on primary frequency control [9], [10]. Despite the fact that an increase in wind power reduces the amount of conventional generation [11], [12], its share is still small as compared with conventional power sources. On the other hand, the impact of wind power penetration on operative reserves related to 'non-event', as shown in Figure 1, is noticeable [6].

V. Sensitivity Analysis

In this section two sensitivity studies are carried out to investigate the behavior of LOLP indicator using the Convolution Method.

A. LOLP Indicator Sensitivity

A sensitivity analysis on the LOLP indicator has been carried out by considering variations on: Operating reserve and time window. Results for the High wind integration scenario are shown in Figure 9.

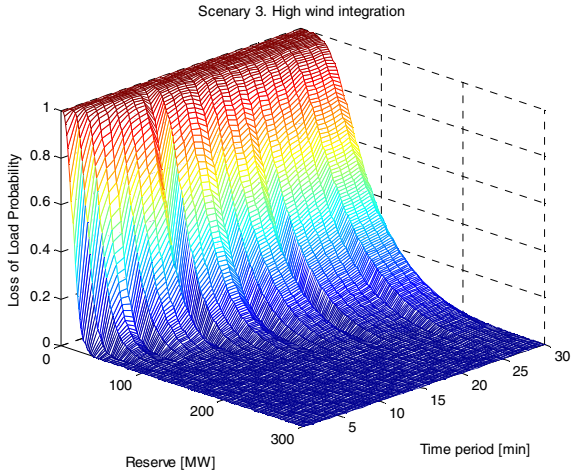

Figure 9. High wind integration LOLP for different time windows.

Figure 9 shows that LOLP increases rapidly when reserve margins decrease below 100 MW. Also, as the time window is increased the reserve margin increases for a given LOLP. These results confirm which has already been reported in the literature.

It is important to highlight that this information is also useful for assessing primary frequency control. In fact, the

LOLP indicator can be estimated through the ratio ΔP/ΔT (ramp of amount of MW required). According to the results of Figure 9, this ratio is 8[MW/min] between 1 and 9 min, 8.9[MW/min] between 10 and 19[min], and 9.4[MW/min] between 20 and 29[min], all cases for a LOLP of 3%. This information can be used to accurately tune the operating reserves.

B. Comparison with Other Methods

In order to compare the performance of different methods that assess the operating reserve, a test was carried out by using the NGIS system. In Table 2, the results for the operating reserve by using different methodologies (see Section II), which are due to wind power fluctuations only (mid wind penetration scenario) are presented.

Table 2. Operative Reserves for Different Methods.

Reserve requirement / Time scale	$R_0[MW]$	LINEAR METHOD $\Delta R_1[MW]$	N-SIGMA METHOD $\Delta R_2[MW]$	CONVOL METHOD (3% LOLP) $\Delta R_3[MW]$
5 min	28.0	67.5	24.6	24.9
10 min	45.4	83.7	30.2	23.1
20 min	77.3	129.1	46.7	33.2
30 min	102.1	206.0	78.0	53.8

Results indicate that the linear method (ΔR_1) and n-sigma method (ΔR_2) render higher values than the proposed Convolution Method.

As the variability of demand and wind fluctuations are not correlated it is expected that the Linear Method overestimates the needs for operating reserve.

On the other hand, predictions rendered by the n-sigma method (with $n = 3$) are higher than those of the Convolution Method. This leads to the conclusion that the operating reserves do not follow a Gaussian probability distribution function. Some authors propose modifying the parameter n (2.5, 4 or 6) depending on the type of reserve to deal with this problem [8]. In the NGIS case, it was found that this could be achieved by using a value between 2.5 and 3, which obtain $\Delta R_2 \approx \Delta R_3$, especially for smaller time windows.

C. Seasonal Sensitivity

Precision on operating reserves is important for small isolated systems, where the cost of having spinning reserve on expensive thermal units may be high as compared to the economic dispatch schedule. In order to investigate the seasonal effect on operating reserves the Convolution Methodology was computed in summer and winter.

Results indicate that seasonal changes are minor in general. The worst case was observed for the time windows of 30[min], where the differences are in the range of 0.5[MW] to 5.4[MW]. Detailed results for this case are shown in Figure 10.

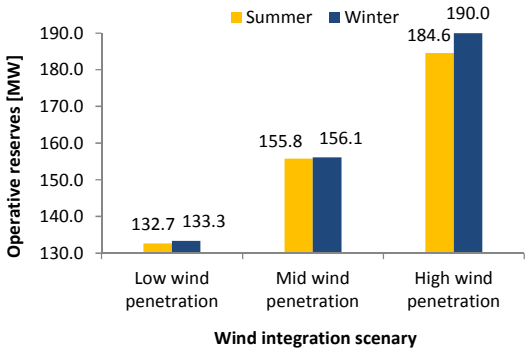

Figure 10. Operating reserves comparison.

VI. Conclusion

This paper proposes a methodology to assess operating reserve in different time frames for wind power penetration scenarios.

The methodology also estimates the LOLP indicator to assess the operative reserve of the system. Results of an application on the expansion plan of a Chilean isolated power system indicate that the methodology is able to estimate operating reserve needs in a time span ranging from 1 to 30 minutes, which adequately satisfy the future needs of this isolated power system.

The methodology may be applied to generate operating reserves by considering any time window, which is constrained only by data availability of sites.

Future work in this line of research is focused on using a more accurate representation for the output power of the wind turbine and testing the precision of the Kaimal approach for turbulences on real sites.

References

[1] T. Ackermann, *Wind power in power systems*.: John Wiley & Sons Ltd., 2005.

[2] Zhe Chen Frede Blaabjerg, *Power electronics for modern wind turbines*.: Morgan & Claypool, 2006.

[3] J. Weatherill, G. Strbac G. N. Bathurst, "Trading wind generation in short term energy markets," *IEEE Transactions on Power Systems*, vol. 17, pp. 782-789, 2002.

[4] Ministerio de Energía, Gobierno de Chile. (2013, May) Explorador de Energía Eólica. [Online]. ernc.dgf.uchile.cl/Explorador/Eolico2/

[5] North American Electric Reliability Corporation, "Reliability Standards for the Bulk Power Systems of North America," Jun 2010.

[6] Brendan Kirby, Eamonn Lannoye, Michael Milligan, Damian Flynn, Bob Zavadil, Mark O'Malley Erik Ela, "Evolution of Operating Reserve Determination in Wind Power Integration Studies," IEEE, 2010.

[7] ENTSO-E. (2009, March) European Network of Transmission System Operators For Electricity. [Online]. https://www.entsoe.eu/fileadmin/user_upload/_library/publications/entsoe/Operation_Handbook/Policy_1_final.pdf

[8] Michael Milligan, Erik Ela, Nickie Menemenlis, Jan Dobschinski, Baryy Rawn, Ricardo J. Bessa, Damian Flynn, Emilio Gómez-Lázaro, Nina K. Detlefsen Hannele Holttinen, "Methodologies to Determine Operating Reserve Due to Increased Wind Power," *IEEE Transactions on Sustainable Energy*, vol. 3, no. 4, pp. 713 - 723, October 2012.

[9] G. Strbac, B. Fox, D. Flynn, R. Slark, S. Rourke, J. Sinner M. O'Malley, "Operating Reserve Requirement as Wind Power Penetration Increases in the Irish Electricity System," Sustainable Energy Authority of Ireland, Report August 2004.

[10] Pedro M. S. Carvalho, Luis A. F. M. Ferreira, Juhua Liu, Bruce H. Krogh, Nipun Popli, Marija D. Ilic By Le Xie, "Wind Integration in Power Systems: Operational Challenges and Possible Solutions," *Proceeding of the IEEE*, vol. 99, no. 1, pp. 214-232, January 2011.

[11] A. Mullane, M. O'Malley G. Lalor, "Frequency Control and Wind Turbine Technologies," *IEEE Transactions on Power Systems*, vol. 20, no. 4, pp. 1905-1913, November 2005.

[12] S.W.H. de Haan, J. A. Ferreira J. Morren, "Primary Power/Frequency Control with Wind Turbines and Fuel Cells," in *IEEE PES General Meeting*, Quebec, June 2006.

[13] X. Bai, K. Clark, G. Jordan, N. Mille, J. Zimberlin R. Piwko, "The Effects of Integrating Wind Power On Transmission System Planning, Reliability and Operations: Report on Phase 2," New York State Energy Research and Development Authority, March 2005.

[14] R. Zavadil, "Wind Integration Study for Public Service Company of Colorado," May 2006.

[15] Enernex Corporation, "Minnesota Wind Integration Study Volume I," November 2006.

[16] R. Barth, H. Brand, B. Hasche, D. Swider, H. Ravn, C. Weber P. Meibom, "All Island Grid Study Workstream 2B: Wind Variability Management Studies," July 2007.

[17] B. Kirby E. Ela, "Lessons Learned NREL Technical Report," ERCOT, NREL/TP-500-43373, July 2008.

[18] M. Huneault, J. Bourret, A. Robitaille N. Menemenlis, "Calculation of balancing reserves incorporating wind power into the Hydro-Québec system over the time horizon of 1 to 48 hours," in *Proceedings 8th International Workshop on Large-Scale Integration of Wind Power Into Power Systems and on Transmission Networks of Offshore Wind Farms*, Bremen, Germany, October 2009.

[19] A. Brand, W.L. Kling M. Gibescu, "Estimation of Variability and Predictability of Large-Scale Wind Energy in the Netherlands," *Wind Energy*, vol. 12, pp. 241-260, 2009.

[20] Enernex Corporation, "Eastern Wind Integration and Transmission Study," NREL, January 2010.

[21] GE Energy, "Western Wind and Solar Integration Study," NREL, NREL/SR-550-47434, May 2010.

[22] Eir Grid and SONI, "All island TSO Facilitation of Renewables Studies," June 2010.

[23] German Energy Agency (Deutsche Energie-Agentur GmbH), "Integration of Renewable Energy Sources in the German Power Supply System from 2015-2020 with an Outlook to 2025," Berlin, November 2010.

[24] A. Robitaille et al., "Preliminary Impacts of Wind Power Integration in the Hydro-Quebec Systm," *Wind Engineering*, vol 36, no 1, 2012.

[25] S. Jachnert, G. L. Doorman, T. Gjengedal T. Aigner, "The Effect of Large-Scale Wind Power on System Balancing in Northern Europe," *IEEE Trans on Sustainable Energy*, vol 3, no 4, pp. 751-759, 2012.

[26] NREL. (2013, May) Dynamic Maps, GIS Data, Analysis Tools. [Online]. www.nrel.gov/gis/wind.html

[27] Consortium for Small-Scale Modelling. (2013, May) Consortium for Small-Scale Modelling. [Online]. www.cosmo-model.org

[28] F.D. Bianchi, H. de Battista, and R.J. Mants, *Wind Turbine Control Systems*.: Springer, 2007.

[29] Madeleine Gibescu, Arno J. Brand Luciano De Tommasi, "A dynamic wind farm aggregate model for the simulation of power fluctuations due to wind turbulence," *Journal of Computational Science*, vol. 1, no. 2, pp. 75-81, March 2010.

[30] N. A. Cutululis, A. Vigueras-Rodríguez, L. E. Jensen, J. Hjerrild, M. H. Donovan, H. Madsen P. Sorensen, "Power fluctuations from large wind farms," *IEEE Trans on Power Systems*, v. 22, no. 3, pp. 958-965, August 2007.

[31] E. Anahua, St. barth, H. Gontier, A.P. Schaffarczyk, D. Kleinhans, R. Friedrich J. Peinke, "Turbulence a Challenging Issue for the Wind Energy Conversion," in *EWEC*, Mûnster, Germany, April 2008.

[32] Pedro Rosas, "Dynamic Influences of Wind Power on the Power System," Oersted Institute, Technical University of Denmark, Lyngby, Denmark, Phd Thesis - Technical Report Riso R-1408 ISBN 87-91184-16-9, 2003.

[33] A.G. Davenport, "The spectrum of horizontal gustiness near the ground in high winds," *Quatrterly Journal of Meteorology Society*, vol. 87, no. 372, pp. 194-211, 1961.

[34] M. Asari, T. Sato, K. Yamaguchi, M. Shibata, T. Maejima T. Nanahara, "Smoothing effects of distributed wind turbines," *Wind Energy*, vol. 7, 2004.

[35] Fernando Borbón Guillén, "Development of a Design Tool for Offshore Wind Farm Layout Optimization," Technische Universiteit Delft, Eindhoven, The Netherlands, Master of Science Thesis 2010.

[36] R. Barthelmie, S. Pryor, O Rathmann, S Larsen, J Hojstrup S. Frandsen, "Analytical Modelling of Wind Speed Deficit in Larga Offshore Wind Farms," *Wiley Interscience - Wind Energy*, vol. 9, pp. 39-53, January 2006.

[37] S. Frandsen, R. Barthelmie O. Rathmann, "Implementation of Turbine Wake Model for Wind Resource Software," in *IEA Workshop on Wake Modelling*, Billund, 2006.

[38] F. Larraín, "Estudio de Integración de las ERNC al SING: Caso Eólico," University of Chile, Santiago, Thesis 2012.

[39] CDEC-SING, "Informe de Expansión Sistema de Transmisión Troncal del SING," CDEC-SING, Santiago, Estudio 2011.

[40] CDEC-SING. (2012, December) System Transmission Operator - North Great Interconnected System. [Online]. www.cdec-sing.cl